Organic Process Research & Development **2009**, *13*, 230–241

Development of a Practical Synthesis of a p38 MAP Kinase Inhibitor

Oliver R. Thiel,*,† Michal Achmatowicz,† Charles Bernard,† Philip Wheeler,† Cecile Savarin,† Tiffany L. Correll,‡ Annie Kasparian,† Alan Allgeier,† Michael D. Bartberger,§ Helming Tan,‡ and Robert D. Larsen†

Department of Chemical Process Research and Development, Department of Molecular Structure and Design, and Department of Analytical Research and Development, Amgen Inc., One Amgen Center Drive, Thousand Oaks, California 91320-1799, U.S.A.

Abstract:

A practical synthesis of the phthalazine-based p38 MAP kinase inhibitor [(*S*)-2] was needed for an ongoing program. Vibrational circular dichroism provided the assignment of the absolute stereochemistry of the target compound. The selected synthetic route for (*S*)-2 required identification of efficient reaction conditions for the construction of carbon−oxygen, carbon−carbon, and carbon−nitrogen bonds to connect the key building blocks. An efficient two-step method (chlorodehydroxylation, aromatic nucleophilic substitution) for the synthesis of arylether [(*S*)-10] was developed. PAT (*in situ* Raman spectroscopy) was utilized to monitor and control the formation of a lithium alkoxide in this reaction. The synthesis of (*S*)-2 was completed using high-yielding Suzuki- and amide-coupling reactions. The isolation conditions for these steps were optimized to obtain material of very high purity without the need for any complicated workup procedures.

Introduction

p38 mitogen-activated protein (MAP) kinases are intracellular serine/threonine kinases that positively regulate the production and action of several pro-inflammatory mediators, specifically the release of tumor necrosis factor-α (TNF-α) and interleukin-1 (IL-1) in response to stress.[1] These cytokines are involved in disease states such as rheumatoid arthritis (RA), Crohn's disease (inflammatory bowel disease), and psoriasis. Biological agents that sequester TNF-α show impressive clinical efficacy in the treatment of these diseases.[2] Small-molecule inhibitors of p38 MAP kinase would be a potential alternative for these biological agents, and the efficacy of these agents has been demonstrated in clinical studies.[3] Our medicinal chemistry team has been pursuing the discovery of p38 MAP kinase inhibitors for several years, and many suitable candidates have been selected for further development. Substantial efforts have focused on highly selective and potent inhibitors that were based on a phthalazine scaffold.[4] A practical synthesis of phthalazine derivative **1** was recently reported by this laboratory,[5] and the current contribution describes the process research and development involved in the large-scale synthesis of the derivative (*S*)-**2** (Figure 1). The two development candidates differ in the 1-substituent of the phthalazine; while the replacement of the morpholine with the chiral trifluoroisopropanol may appear to be only a minimal change, from a synthetic perspective, it resulted in very different chemical and physicochemical behavior of the intermediates that required significant process development efforts.

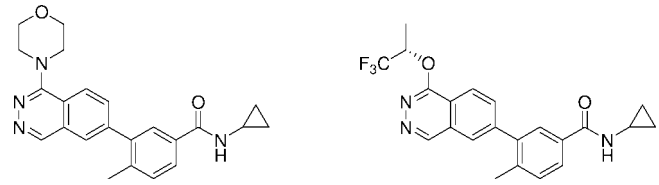

1 (*S*)-2

Figure 1. **p38 MAP kinase inhibitors 1 and (*S*)-2.**

The synthesis that was employed by our medical chemistry team is shown in Scheme 1.[4] 2-Chloro-6-bromophthalazine (**3**)[6] was reacted with the sodium alkoxide derived from 1,1,1-trifluoropropan-2-ol [(±)-**9**] (3 equiv) in a mixture of THF and DMF to afford ether **4** in a racemic fashion. This aryl bromide was subjected to a Suzuki-coupling with pinacol ester **5**[7] to afford the target compound (±)-**2** in good yield. The desired enantiomer of this compound was obtained by chiral preparative chromatography (SFC with Chiralpak AD). This approach led to an undetermined absolute stereochemistry of **2**, making this a key issue prior to initiation of further synthetic efforts.

This first-generation synthesis suffered from the limited availability of the building blocks **3** and **5**. Furthermore, the need for a chromatographic resolution in the preparation of the desired enantiomer made the yields and efficiency of this synthesis low. To support the program we required an efficient synthesis of (*S*)-**2** that would enable production of kilogram quantities.

* To whom correspondence should be addressed: Telephone: 805-447-9520. Fax: 805-375-4532. E-mail: othiel@amgen.com.
† Department of Chemical Process Research and Development.
‡ Department of Analytical Research and Development.
§ Department of Molecular Structure and Design.

(1) Chen, Z.; Gibson, T. B.; Robinson, F.; Silvestro, L.; Pearson, G.; Xu, B.; Wright, A.; Vanderbilt, C.; Cobb, M. H. *Chem. Rev.* **2001**, *101*, 2449.
(2) Etanercept, infliximab, and adalimumab are TNF-α blockers currently approved in the United States and elsewhere for various inflammatory diseases.
(3) (a) Gaestal, M.; Mengel, A.; Bothe, U.; Asadullah, K. *Curr. Med. Chem.* **2007**, *14*, 2214. (b) Peifer, C.; Wagner, G.; Laufer, S. *Curr. Top. Med. Chem.* **2006**, *6*, 113. (c) Margutti, S.; Laufer, S. A. *ChemMedChem* **2007**, *2*, 1116.
(4) Herberich, B.; Cao, G.-Q.; Chakrabarti, P. P.; Falsey, J. R.; Pettus, L.; Rzasa, R. M.; Reed, A. B.; Reichelt, A.; Sham, K.; Thaman, M.; Wurz, R. P.; Xu, S.; Zhang, D.; Hsieh, F.; Lee, M. R.; Syed, R.; Li, V.; Grosfeld, D.; Plant, M. H.; Henkle, B.; Sherman, L.; Middleton, S.; Wong, L. M.; Tasker, A. S. *J. Med. Chem.* **2008**, *51*, 6271.
(5) Achmatowicz, M.; Thiel, O. R.; Wheeler, P.; Bernard, C.; Huang, J.; Larsen, R. D.; Faul, M. M. *J. Org. Chem.* **2009**, *74*, 795.
(6) Obtained in four steps (45% overall yield) from 4-bromo-2-methylbenzonitrile.
(7) Prepared in two steps from 3-iodo-4-methylbenzoic acid, utilizing a palladium-catalyzed boron−carbon formation.

10.1021/op800250v CCC: $40.75
Published on Web 01/15/2009

Scheme 1. **Medicinal chemistry synthesis of (*S*)-2**

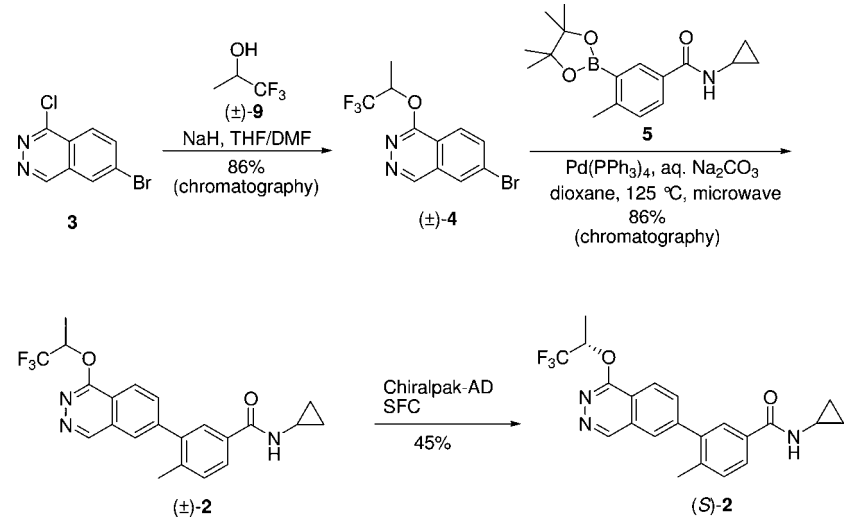

Scheme 2. **Retrosynthesis of (*S*)-2**

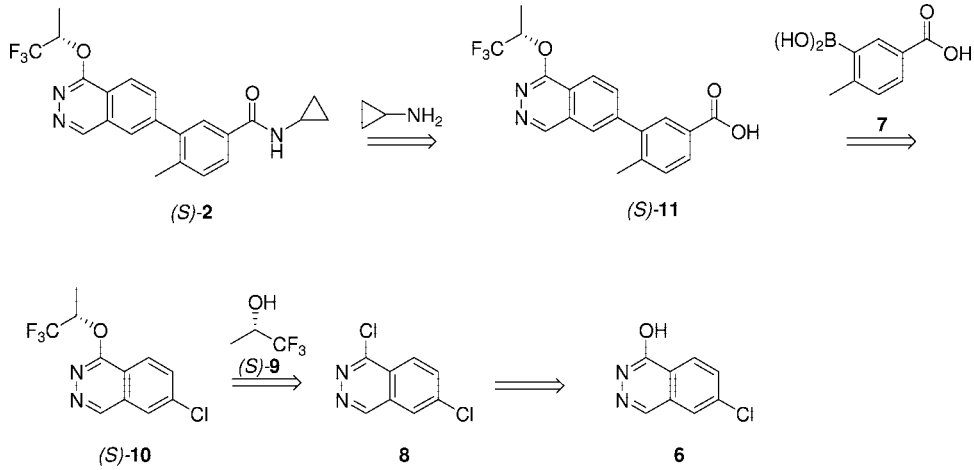

Earlier development work for the synthesis of **1** had provided access to building blocks **6** and **7**,[5] which we decided to leverage for the synthesis of **2** (Scheme 2). We envisaged converting 6-chlorophthalazin-1-ol (**6**) into 1,6-dichlorophthalazine (**8**), followed by displacement with the enantiomerically pure alcohol (*S*)-**9** to obtain the key building block (*S*)-**10**. Suzuki-coupling with boronic acid **7** followed by amide-coupling with cyclopropylamine should allow access to the target compound. Several key developmental challenges were identified in this proposed synthetic sequence. The formation of arylether (*S*)-**10** would require scaleable reaction conditions, which avoid potential side reactions that are associated with the chlorophthalazine scaffold.[5] The Suzuki-coupling of aryl chloride (*S*)-**10** was expected to require an extensive screen of reaction conditions to obtain a high yield in the formation of this key bond. In addition to these purely synthetic organic challenges significant challenges in the physicochemical properties of the intermediates were encountered. Upon switch from the racemic to the enantiopure series a significant decrease in the solubility of the key intermediates forced us to redesign the isolation procedures.

The synthetic approach to the phthalazine core **6** leveraged the inherent symmetry of the starting material (Scheme 3). Reaction of 4-chlorobenzoyl chloride with *tert*-butylamine led to the corresponding amide. Selective ortho metalation using methyllithium followed by quench with *N*,*N*-dimethylformamide afforded **12** without incident. This hydroxyisoindolinone was transformed to 6-chlorophthalazin-1-ol (**6**) using hydrazine hydrate in acetic acid. Overall, this synthetic sequence could be readily scaled up, and a good overall yield was obtained on kilogram scale.[5] The boronic acid **7** was obtained from 3-iodo-4-methylbenzoic acid through a one-pot process. The carboxylic acid functionality was deprotonated without concomitant reduction of the iodide using isopropylmagnesium chloride below −50 °C. A second equivalent of the Grignard reagent was used to effect a clean magnesium−iodine exchange, and the resulting arylmagnesium species was trapped with triisopropyl borate. Acidic hydrolysis followed by crystallization from THF/heptane allowed access to **7** in acceptable yield.[5]

Results and Discussion

Determination of Absolute Stereochemistry. At the outset of our development work, the absolute configuration of the more active enantiomer of **2** had not been determined. Initially we were able to procure only (±)-1,1,1-trifluoropropan-2-ol [(±)-**9**], which gave rise to compound (±)-**10** and subsequent products as mixtures of enantiomers. Thus, it was of interest to determine the absolute stereochemistry of the active form of **2**

Scheme 3. **Synthesis of building blocks 6 and 7**

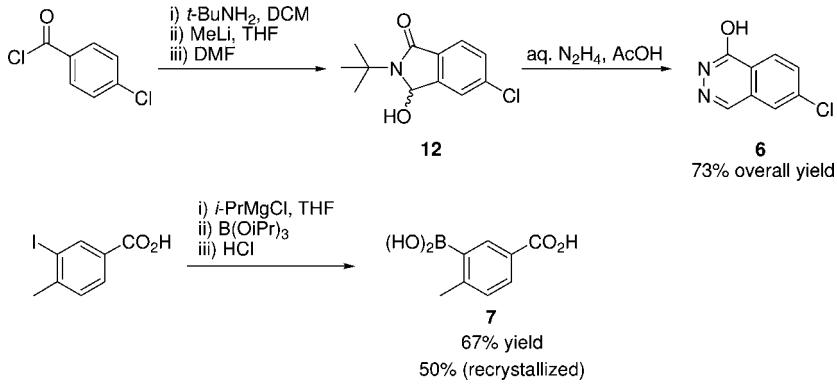

in order to facilitate selective synthesis of the more potent stereoisomer. Single X-ray crystallography was not directly available for assignment due to the lack of heavy-atom containing intermediates.

Vibrational circular dichroism (VCD)[8] has emerged as a reliable and efficient method for the determination of absolute stereochemistry of chiral molecules in solution without the need for crystalline material as required by X-ray crystallography. Comparison of the experimental VCD spectra of each enantiomer (necessarily mirror images) to those obtained via quantum mechanical calculations[9] for a defined stereochemical configuration provides an absolute assignment. Species **10** was chosen for VCD determination due to its ease of chiral separation and small size, the latter allowing fast computational spectral determination and affording a simplified conformational landscape. Reaction of 1,6-dichlorophthalazine (**8**) with the lithium alkoxide of (±)-**9** afforded (±)-**10** (*vide infra* for more details about the reaction conditions). After separation of the enantiomers by chiral preparative chromatography (Chiralpak AD-H, hexane/2-propanol 95:5) the VCD spectra of both enantiomers, **10a** (t_R = 5.4 min) and **10b** (t_R = 6.2 min), were acquired on a BioTools Dual PEM Chiral IR instrument. Conformational ensembles of (*R*)- and (*S*)-**10** were obtained via stochastic search using the MMFF94 force field,[10] followed by geometry optimization and harmonic frequency and VCD rotational strength determination with the B3LYP hybrid density functional and 6-31G* basis set.[11] The predicted VCD (line) spectra for the three resultant, unique conformations were convolved using a Lorentzian function, followed by Boltzmann weighting based on the predicted relative free energy of each conformation to yield a final predicted VCD spectrum for each enantiomer. Comparison of the theoretical spectra with those obtained experimentally led to the unambiguous assignment of stereoisomer **10a** (see Figure 2) as (*S*)-**10**. The use of this compound in the remaining synthetic steps coupled with chiral HPLC analysis (Chiralpak AD-H) led to the assignment of **2** as the (*S*)-enantiomer.

The VCD assignment was subsequently confirmed by chemical synthesis (Scheme 4). Racemic 2-(trifluoromethyl)oxirane [(±)-**12**] was subjected to Jacobsen's hydrolytic kinetic resolution using (*R,R*)-Co(salen) as catalyst leading to enantiomerically enriched (*S*)-2-(trifluoromethyl)oxirane [(*S*)-**13**].[12,13] Reductive ring-opening with lithium aluminum hydride afforded (*S*)-**9** which upon reaction with 1,6-dichlorophthalazine (**8**), prepared by the same method as reported in the synthesis of **1**,[5] led to the intermediate (*S*)-**10**, the chiral HPLC retention time of which was identical with that of **10a**, thereby corroborating the predicted stereochemical assignment mentioned

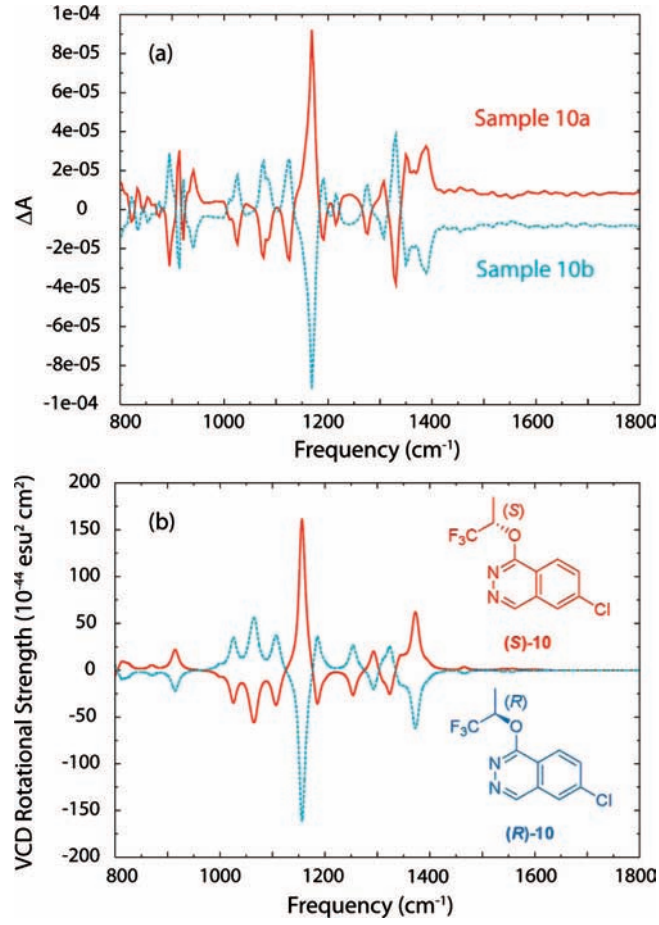

Figure 2. **Solvent-subtracted experimental (a) and theoretical (b) VCD spectra for (*R*)- and (*S*)-10.**[15]

(8) (a) Stephens, P. J.; Devlin, F. J.; Pan, J. *Chirality* **2008**, *20*, 643. (b) Freedman, T. B.; Cao, X.; Dukor, R. K.; Nafie, L. A. *Chirality* **2003**, *15*, 734.

(9) (a) Devlin, F. J.; Stephens, P. J.; Cheeseman, J. R.; Frisch, M. J. *J. Phys. Chem. A* **1997**, *101*, 6322. (b) Devlin, F. J.; Stephens, P. J.; Cheeseman, J. R.; Frisch, M. J. *J. Am. Chem. Soc.* **1996**, *118*, 6327. (c) Cheeseman, J. R.; Frisch, M. J.; Devlin, F. J.; Stephens, P. J. *Chem. Phys. Lett.* **1996**, *252*, 211.

(10) (a) Halgren, T. A. *J. Comput. Chem.* **1999**, *20*, 730. (b) The MMFF94 conformational search was performed with the *Molecular Operating Environment (MOE)*, v. 2007.09; Chemical Computing Group Inc.: Montreal, Canada, 2007; http://www.chemcomp.com.

Scheme 4. **Stereochemical assignment by the enantioselective synthesis of (*S*)-10**

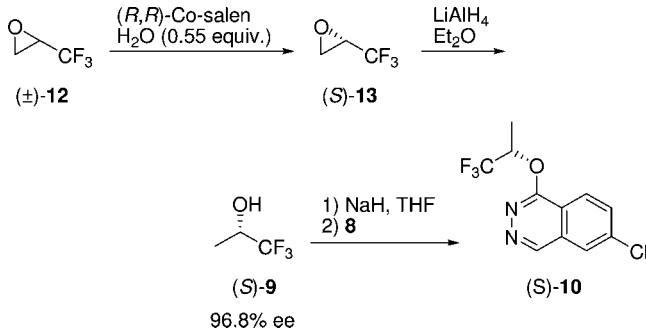

above.[14] In conclusion, both methods are complementary. In this particular application the assignment using chemical synthesis was relatively straightforward (two synthetic steps), and it required similar resources compared to the VCD method. In systems where intermediates of known absolute stereochemistry are not as easily available, however, VCD can offer distinct advantages.

Formation of Carbon−Oxygen Bond through Aromatic Nucleophilic Substitution. The medicinal chemistry route involved nucleophilic aromatic substitution of **3** using the sodium alkoxide derived from 1,1,1-trifluoropropan-2-ol [(±)-**9**]. A brief investigation in reversal of nucleophile and electrophile was undertaken, since it would obviate the need for an activation of **6** with phosphorous oxychloride. Tosylate **14**[16] and mesylate **15** were prepared as alkylating agents starting from (*R*)-1,1,1-trifluoropropan-2-ol [(*R*)-**9**] (Figure 3).[17] However, all attempts to effect the *O*-alkylation of **6** using these substrates under literature conditions (LHMDS in THF; K_2CO_3 in acetone; NaH in DMF)[18] failed to produce even a trace amount of (*S*)-**10**; typically, no conversion was observed. At higher temperatures (55−60 °C), generation of multiple unidentified products, resulting presumably from the decomposition of the alkylating agent, were observed. Since the direct *O*-alkylation of **6** was not successful, development of the S_NAr route using (*S*)-**9** and **8** as nucleophilic and electrophilic partners, respectively, was explored (Scheme 5).

Figure 3. **Potential alkylating agents 14 and 15.**

Scheme 5. **S_NAr route to (*S*)-10**

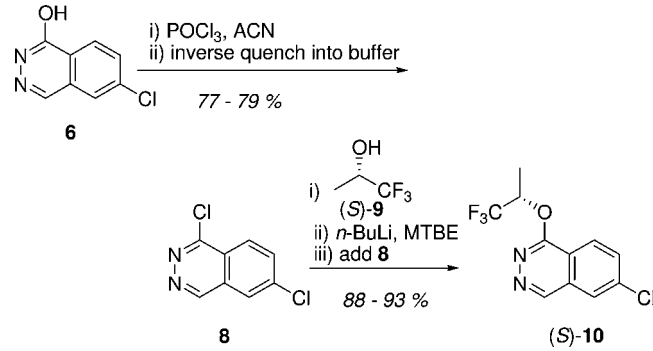

1,6-Dichlorophthalazine (**8**) had been an intermediate in the synthesis of **1**.[5] The chlorodehydroxylation of **6** was performed in chlorobenzene, followed by dilution with dichloromethane and an aqueous NaOH quench. Initially, **8** was isolated as a wet solid from the organic solution after solvent evaporation. It was observed that this intermediate has some inherent stability issues. Exposure to aqueous acidic conditions led to hydrolysis and reversion to **6**, whereas under anhydrous conditions dimerization and oligomerization reactions took place in the presence of Lewis or Brønsted acids. Due to these instability concerns, a through-process was preferred in which **8** was not isolated but carried crude to the next step (nucleophilic aromatic substitution with morpholine). Although this through-process was successfully executed on a kilogram scale for the synthesis of **1**, it was not optimal. The major concerns for the synthesis of **8** that were to be addressed were as follows: (i) the potential for a delayed exotherm during the quench, (ii) the use of chlorinated solvents, and (iii) the lack of a control point.

Early on during development of the chlorodehydroxylation of **6**, it was noted that acetonitrile could be a viable solvent for this transformation (complete conversion, 69% isolated yield of **8**). However, difficulties with a reproducible isolation of the hydrolytically labile **8** from the water-miscible acetonitrile initially discouraged further experiments. It was then conceived that a quench and isolation from a buffered aqueous media could mitigate the stability issues and therefore this approach warranted revisiting.[19] The chlorodehydroxylation reaction was performed with 1.5 equiv of $POCl_3$ in acetonitrile at 80 °C, and upon complete conversion, the reaction mixture was quenched inversely, so that the reaction mixture was transferred into an aqueous phosphate buffer solution with concomitant adjustment to pH 6.8−8.0 using 2 N aqueous NaOH while maintaining the temperature below 30 °C. The product could

(11) All density functional theory calculations were performed with the *Gaussian 98* program system. Frisch, M. J.; Trucks, G. W.; Schlegel, H. B.; Scuseria, G. E.; Robb, M. A.; Cheeseman, J. R.; Zakrzewski, V. G.; Montgomery, J. A., Jr.; Stratmann, R. E.; Burant, J. C.; Dapprich, S.; Millam, J. M.; Daniels, A. D.; Kudin, K. N.; Strain, M. C.; Farkas, O.; Tomasi, J.; Barone, V.; Cossi, M.; Cammi, R.; Mennucci, B.; Pomelli, C.; Adamo, C.; Clifford, S.; Ochterski, J.; Petersson, G. A.; Ayala, P. Y.; Cui, Q.; Morokuma, K.; Malick, D. K.; Rabuck, A. D.; Raghavachari, K.; Foresman, J. B.; Cioslowski, J.; Ortiz, J. V.; Stefanov, B. B.; Liu, G.; Liashenko, A.; Piskorz, P.; Komaromi, I.; Gomperts, R.; Martin, R. L.; Fox, D. J.; Keith, T.; Al-Laham, M. A.; Peng, C. Y.; Nanayakkara, A.; Gonzalez, C.; Challacombe, M.; Gill, P. M. W.; Johnson, B. G.; Chen, W.; Wong, M. W.; Andres, J. L.; Head-Gordon, M.; Replogle, E. S.; Pople, J. A. *Gaussian 98*, Rev. A.11.3; Gaussian, Inc.: Pittsburgh, PA, 2002.

(12) Schaus, S. E.; Brandes, B. D.; Larrow, J. F.; Tokunaga, M.; Hansen, K. B.; Gould, A. E.; Furrow, M. E.; Jacobsen, E. N. *J. Am. Chem. Soc.* **2002**, *124*, 1307.

(13) The absolute stereochemistry for this substrate was assigned by Jacobsen et al. by comparison of the optical rotation with earlier data in Ramachandran, P. V.; Gong, B.; Brown, H. C. *J. Org. Chem.* **1995**, *60*, 41.

(14) After the completion of the synthesis of (*S*)-**2** the absolute stereochemistry was independently confirmed by a single-crystal structure of (*S*)-**2** in the active site of p38-kinase.

(15) Resolution of 8 cm^{-1} and Lorentzian half-widths for experimental and theoretical plots, respectively. B3LYP/6-31G* frequencies scaled by 0.96.

(16) Hanack, M.; Ullman, J. *J. Org. Chem.* **1989**, *54*, 1432.

(17) The (*R*)-enantiomer of the chiral alcohol is also commercially available, albeit in lower stereochemical purity (92−94% ee).

(18) (a) Cui, P.; Macdonald, T. L.; Chen, M.; Nader, J. L. *Bioorg. Med. Chem. Lett.* **2006**, *16*, 3401. (b) Baraldi, P. G.; Tabrizi, M. A.; Preti, D.; Bovero, A.; Romagnoli, R.; Fruttarolo, F.; Zaid, N. A.; Moorman, A. R.; Varani, K.; Gessi, S.; Merighi, S.; Borea, P. A. *J. Med. Chem.* **2004**, *47*, 1434.

be isolated by simple filtration from the quench mixture (solubility of **8** in mother liquors: <0.5 mg/mL). Prolonged heating with $POCl_3$ (12−14 h), inverse quench at up to 40 °C, and aging of the quenched aqueous mixture at pH 7−11 (12−14 h) had no adverse effects on the purity of **8** (>96%).

The procedure thus developed was successfully performed on kilogram scale. After complete conversion of **6** (<2%) was observed after 3 h at 80 °C, the inverse quench was performed over 4 h, during which the pH was maintained in the desired range (6.8−8.0). The precipitated materials were collected by filtration and rinsed with water twice. The filter cake was dried under a stream of nitrogen to afford **8** in good yield (79% corrected yield, 96.2% purity, 87.0 wt %). The relatively low potency of this material could be accounted for by the presence of water (0.2% weight loss by TGA) and inorganic salts (1.7 wt % chloride and 0.3 wt % phosphate by ion chromatography) as well as some oligomeric and polymeric byproducts. These impurities were efficiently removed during a polishing filtration operation in the next reaction.

The subsequent synthetic step was to substitute the chiral fragment for the newly introduced chloride in **8**. Initially only racemic 1,1,1-trifluoropropan-2-ol (±)-**9** was available, but during our development work we were able to identify Julich/Codexis and DSM as large-scale suppliers of (*S*)-**9**. This chiral alcohol could be obtained in high enantiomeric purity (>99.0% ee) by reduction of 1,1,1-trifluoroacetone using alcohol dehydrogenases,[20] whole cell yeast,[21] or a chiral ruthenium catalyst.[22] For ease of isolation of the low-boiling liquid (bp 81 °C), the alcohol is obtained as a solution in an organic solvent. For our intended use, a solution of MTBE (35−64 wt % by ^{1}H NMR) was deemed appropriate, since MTBE is chemically inert under most reaction conditions that can be envisioned for a nucleophilic aromatic substitution. After initial development work was completed with (±)-**9**, the switch to (*S*)-**9** was attempted; however, significant changes in the physicochemical properties (crystallinity and solubility) of the intermediates resulted, which raised the need to redesign their isolation as discussed later.

While the medicinal chemistry synthesis had employed sodium hydride for the deprotonation of (±)-**9**, handling and safety issues made the use of a soluble base desirable. The lithium alkoxide of (±)-**9** could be prepared in THF by treatment of the alcohol (1.5 equiv) with 1.4 equiv of *n*-butyllithium in hexane. Aromatic nucleophilic substitution of the chloride of **8** (limiting reagent) proceeded cleanly at room temperature over 1−2 days (≥98% conversion), affording racemic ether (±)-**10**. After an aqueous workup and filtration through a short plug of silica, the product could be isolated in reasonable yield (66−76%). Without affecting purity, the reaction time was reduced from 1−2 days to 2−3 h by heating to reflux. Replacing THF by MTBE led to a further improvement as the reaction rate in the MTBE/hexane system turned out to be faster, reducing the reaction time to 1.0−1.5 h at reflux (48−56 °C). In an optimized procedure, the reaction mixture (approximately 12 vol of 2:1 v/v of MTBE/hexanes) was quenched with a mixture of saturated aqueous sodium chloride and ammonium chloride (1:1 v/v, 10 vol). After filtration, the layers were separated, and the organic layer was washed with water (5 vol). The reaction solvents were replaced by EtOH (10 vol) through vacuum distillation. Water (10 vol) was added to the ethanol solution slowly at 40 °C, and the resulting suspension was kept at 20 °C for 30 min. Filtration then afforded (±)-**10** in 78% yield (>98% purity).

On the basis of the reaction conditions that were developed for (±)-**9** further optimization was conducted using (*S*)-**9** as a solution in MTBE (35−64 wt %). The stoichiometry and quality of the organolithium reagent used in the deprotonation was of critical importance. Using excess *n*-butyllithium led to formation of 1-butoxy-6-chlorophthalazine and an unidentified impurity. The formation of 1-butoxy-6-chlorophthalazine (up to 33% in product) was likely due to the presence of lithium *n*-butoxide formed by partial oxidation of *n*-butyllithium through traces of air. In contrast, excess of (*S*)-**9** relative to the organolithium reagent was well tolerated in the reaction, and no impact on product purity or isolated yield was observed. In order to control the stoichiometry between (*S*)-**9** and *n*-butyllithium, catalytic 1,10-phenanthroline (0.1−0.4 mol %) was used as an internal indicator during the preparation of the lithium alkoxide. The colorless solution became light yellow during addition of *n*-butyllithium and eventually turned dark brown at the equivalence point. An additional charge of (*S*)-**9** (0.1 equiv) and a corresponding color change back to yellow ensured that no excess organolithium was present in the subsequent step.

A range-finding study on the stoichiometry of the alkoxide relative to **8** was performed. It was found that 1.1 equiv (*S*)-**9** of was sufficient for a complete conversion of **8** possessing high purity (isolated by crystallization from dichloromethane/heptane). However, due to a relatively high level of inorganic and polymeric content (10−15 wt %) in representative batches of **8**, 1.5 equiv of (*S*)-**9** was preferentially used to ensure complete conversion. At least 20 wt % of inorganics (NaCl, Na_2HPO_4 and/or NaH_2PO_4) were tolerated under these conditions. In the absence of alkoxide, **8** slowly reacted with **6**[23] to produce a dimeric side-product with MS 343. Two possible structures for MS 343 were postulated: *N*-arylated dimer **16** or symmetric ether **17** (Scheme 6). The structure of the byproduct was assigned as **16** based on NMR studies and additional data.[24]

The stability of the alkoxide solution in MTBE/hexanes was assessed using a quantitative GC assay with dodecane and MTBE as internal standards. No significant degradation was detected analytically in samples that had been aged for 4 days at room temperature. Side-by-side etherification reactions were performed with a freshly prepared solution of the alkoxide and the same alkoxide

(19) Frey, L. F.; Marcantonio, K.; Frantz, D. E.; Murry, J. A.; Tillyer, R. D.; Grabowski, E. J. J.; Reider, P. J. *Tetrahedron Lett.* **2001**, *39*, 6815.

(20) (a) Rosen, T. C.; Feldmann, R.; Dünkelmann, P.; Daussmann, T. *Tetrahedron. Lett.* **2006**, *47*, 4803. (b) Doderer, K.; Gröger, H.; May, O. Method for the production of enantiomerically enriched 1,1,1-trifluoroisopropanol. Ger. Patent DE102005054282, 2005.

(21) (a) Bucciarelli, M.; Forni, A.; Moretti, I.; Torre, G. *Synthesis* **1983**, 897. (b) Doswald, S.; Hanlon, S. P.; Kupfer, E. Asymmetric reduction of 1,1,1-trifluoroacetone. U.S. Patent Appl. 2007/0009999, 2007.

(22) (a) Sterk, D.; Stephan, M.; Mohar, B. *Org. Lett.* **2006**, *8*, 5935. (b) Puentener, K.; Waldmeier, P. Asymmetric hydrogenation of 1,1,1-trifluoroacetone. WO2008012240, 2008.

(23) Usually present in 1−4% in typical batches of **8**.

(24) Two mono-Suzuki products (MS 443) resulting from a coupling of MS 343 with **7** were detected during the reaction which later converted into a single bis-Suzuki product (MS 543). This observation is consistent only with the unsymmetrical dichloride **16**.

Scheme 6. **Formation of side product 16 as a result of the undercharge of alkoxide**

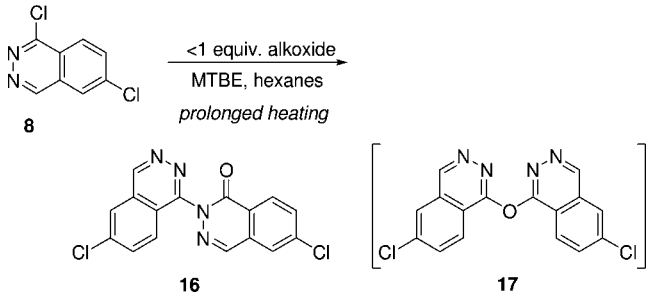

solution except for being aged at room temperature for a day. The assay yield of (*S*)-**10** in this set of experiments was within experimental error (88−91%). Additional ^{19}F NMR experiments with α,α,α-trifluorotoluene as an internal standard showed a partial degradation of the alkoxide solution in the presence of 10 mol % excess *n*-butyllithium over 24 h. In summary, the alkoxide solution appears to be sufficiently thermally stable at room temperature provided that excess *n*-butyllithium is promptly destroyed using excess (*S*)-**9**.

PAT-Application for Monitoring Alkoxide Formation. As previously described, the deprotonation of (*S*)-**9** to generate the lithium alkoxide was monitored at bench scale by the use of an internal colorimetric indicator (1,10-phenanthroline). However, concerns regarding contamination with phenanthroline decomposition products[25] led to pursuit of an *in situ* spectroscopic method which also served to eliminate the need to titrate the *n*-BuLi. *In situ* Raman spectroscopy was ultimately used to monitor the deprotonation of (*S*)-**9** and concomitant formation of the corresponding lithium alkoxide. On the basis of reference spectra, features indicative of C−O stretching or deformation at ∼780 cm^{-1} and ∼792 cm^{-1} were chosen as strong markers for the alkoxide and alcohol, respectively. These features were free from spectral interference by the reaction solvent (MTBE). At bench scale, *in situ* spectra were acquired by the use of a dispersive Raman spectrometer (Raman Rxn 1 Analyzer, Kaiser Optical Systems, Ann Arbor, MI) with incident radiation at 785 nm coupled to a filtered probe head and Hastelloy immersion optic. A custom-built *Pilot E* probe in conjunction with a Raman Rxn 3 analyzer (Kaiser Optical Systems, Ann Arbor, MI) was used for in-process control at a kilogram scale. Reaction completion was determined by monitoring the running relative standard deviation of spectra acquired at 1-min intervals. Figures 4 and 5 show the spectral region of interest recorded as *n*-butyllithium was being charged. The deprotonation of the alcohol as evidenced in the spectra at ∼792 cm^{-1} is kinetically fast, and no delay in the spectral changes relative to addition was observed. Since an excess of *n*-butyllithium resulted in side reactions in the subsequent step and excess (*S*)-**9** was well tolerated in the subsequent chemistry, a small recharge of (*S*)-**9** was performed to ensure that no excess alkyllithium was present. The results obtained by *in situ*

(25) Decomposition of the charge-transfer complex into multiple unidentified products was detected.
(26) Solubilities of (*S*)-**10** vs (±)-**10** at rt (respectively): 68 vs 133 mg/mL in MTBE and 9 vs 14 mg/mL in EtOH/water (2:1 v/v).

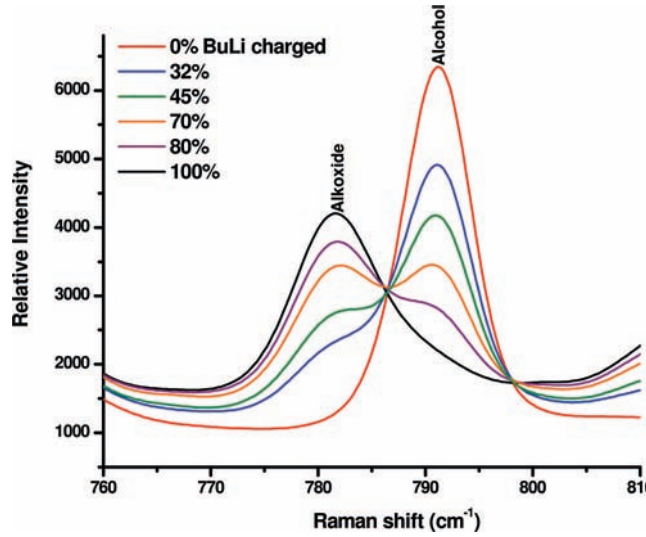

Figure 4. **An overlay of raw in-process spectra acquired to monitor the conversion of (*S*)-9 into its lithium alkoxide during kilogram-scale manufacturing.**

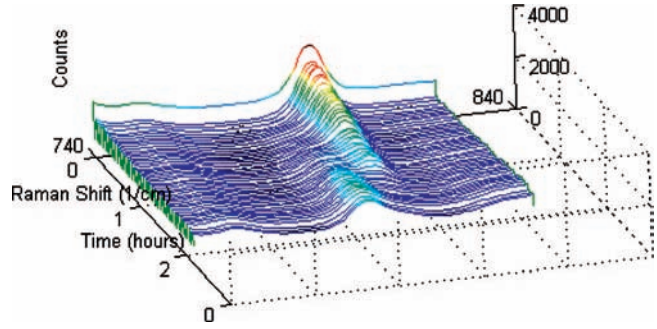

Figure 5. **Typical waterfall plot monitored during *in situ* spectroscopic in process control.**

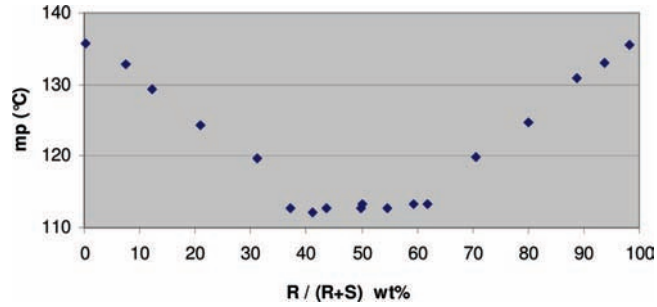

Figure 6. **Melting point of 10 depending on its enantiomeric composition.**

spectroscopy were ascertained by performing an off-line 1,10-phenanthroline check on an aliquot of the alkoxide solution.

A revised workup and isolation protocol had to be developed for the isolation of (*S*)-**10**, since it displayed a much lower solubility compared to that of (±)-**10**.[26] Aqueous ethanol was selected as the solvent for the isolation of **10** as good recovery (>90% yield) and rejection of impurities (>99.0% purity) could be ensured. In the optimized procedure, the alkoxide solution was prepared at 10−25 °C by addition of 2.5 M *n*-butyllithium in hexanes to a solution of (*S*)-**9** in MTBE (1.45 equiv). The deprotonation was monitored by Raman spectroscopy as shown in Figure 4, and after reaching the equivalence point, an additional amount of (*S*)-**9** (0.10 equiv) was added. The preformed alkoxide solution was added to a suspension of **8** in

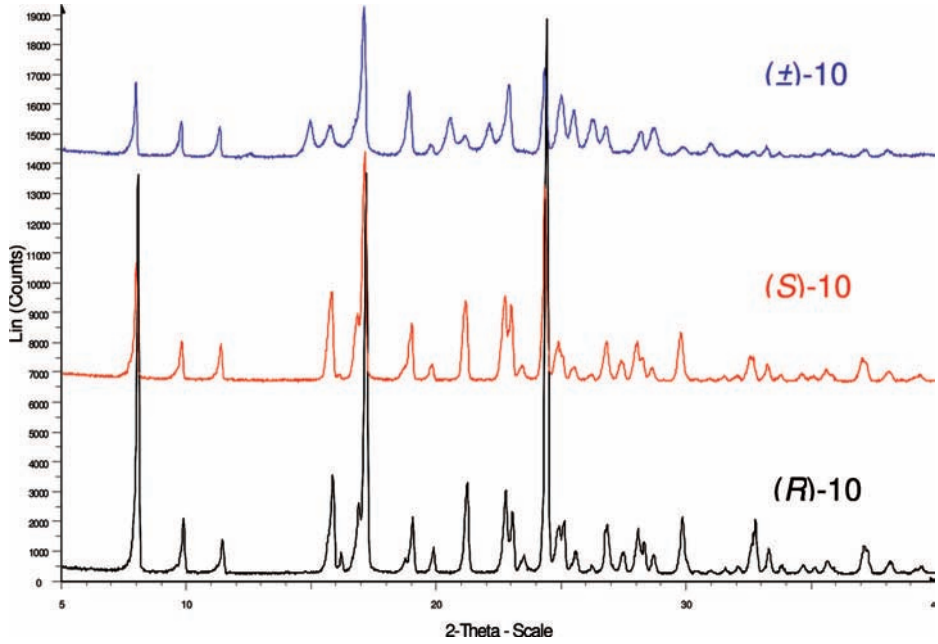

Figure 7. **XRPD-pattern of (±)-10 and single enantiomers of 10.**

MTBE, and the reaction mixture was heated to reflux with complete conversion being observed within 2 h (<0.2% **8**). The reaction mixture was cooled to room temperature and diluted with THF to assist complete dissolution of the product. After quenching with an aqueous ammonium chloride solution, a polish filtration was performed through a Celite pad to remove insoluble inorganic and polymeric impurities. A crude organic solution of (*S*)-**10** (>95% assay yield) was obtained after phase cut. A distillative solvent switch to ethanol was performed (<5.0 wt % THF, <1.0 wt % MTBE), and the product was crystallized by addition of water at 55−65 °C followed by cooling to rt. On filtration, (*S*)-**10** was isolated in high purity (loss to mother liquors: ~ 8 mg/mL; 90−95% isolated corrected yield; >99.5% purity).

Characterization of Solid-State Properties of 10. Although (*S*)-**9** of high enantiomeric purity had been procured, we explored the possibility of using material of lower enantiomeric excess for subsequent campaigns. The decreased solubility of (*S*)-**10** as compared to that of (±)-**10** offered a potential for an ee upgrade at this stage. Applying the standard reaction and isolation conditions, we were able to obtain (*S*)-**10** of relatively high purity (97.4% ee) from (*S*)-**9** of 88.4% ee.

Since the procurement of (*S*)-**9** of lower ee would be of interest from a cost-of-goods perspective, we were interested in defining the type of racemate (conglomerate, racemic compound, or solid solution) that **10** forms.[27] Solid samples with different enantiomeric excesses were prepared by dissolution of varying amounts of (*R*)- and (*S*)-**10** in ethanol followed by evaporation. The recovered solids were analyzed by differential scanning calorimetry and chiral HPLC. The melting point curve (Figure 6) indicates a eutectic point close to a mole fraction (x) of 0.5 (ee = 0%). Interestingly, the melting point of **10** shows only very small variation (<2.0 °C) over a relatively wide range of x (0.37−0.62). (±)-**10** shows a distinct

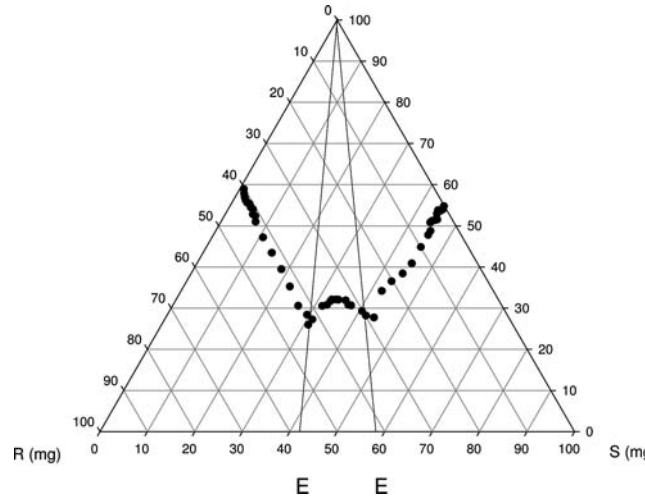

Figure 8. **Ternary phase diagram of enantiomers of 10 in EtOH/water (2:1 v/v).**

X-ray powder diffraction pattern (XRPD) compared to the enantiopure compounds, (*S*)-**10** and (*R*)-**10** (Figure 7). Together this data suggest that the racemate is either a conglomerate with a polymorphic form different from the enantiomers of **10** or a racemic compound with a eutectic point that is relatively close to $x = 0.5$. To differentiate between these two possibilities, conversion experiments in which mixtures of (*S*)-**10** and (±)-**10** were slurried at elevated temperature followed by XRPD analysis of the recovered solids were performed. The patterns corresponded to those recorded for simple mixtures of the two starting materials, suggesting that the racemate crystallizes as a racemic compound. To confirm this hypothesis, a ternary phase diagram (TPD) for the enantiomers of **10** in ethanol/water (2:1) was constructed. Different mixtures of (*R*)- and (*S*)-**10** were equilibrated in that solution for 24 h at room temperature, and the solubility for the individual enantiomers was determined by chiral HPLC as plotted in Figure 8. While deviations from the expected perfect symmetry can be explained by the variability of the solubility assay using the high-throughput

(27) (a) Chen, A. M.; Wang, Y.; Wenslow, R. M. *Org. Process Res. Dev.* **2008**, *12*, 271. (b) Coquerel, G. *Enantiomers* **2000**, *5*, 481. (c) Collet, A. *Enantiomers* **1999**, *4*, 157.

Scheme 7. **PTC conditions for etherification of 8 with (*S*)-9**

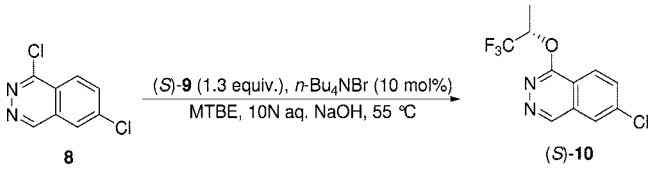

method,[28] the TPD shows that the eutectic point for **10** is at $x = 0.43$, corresponding to an ee of 14%. This result clearly demonstrates that the racemate of **10** is a racemic compound, and it highlights that the TPD provides a more sensitive method to differentiate conglomerate from racemic compound, compared to the melting point diagram. The solid-state properties of (*S*)-**10** have made it an ideal candidate for upgrade of its enantiomeric purity by crystallization as any mixture of **10** with >14% ee can be upgraded to enantiopure material by proper choice of crystallization conditions.

The ether formation under the predefined conditions performed well on scale, but interest remained to conduct the reaction without the use of an alkyllithium reagent. An attractive alternative to the current process is the phase transfer catalysis (PTC) etherification using alcohol (*S*)-**9** and aqueous base. The PTC conditions were successfully applied on laboratory scale using **8**, (*S*)-**9** (1.3 equiv), and cat. Aliquat 100-S (aq tetra-*n*-butylammonium bromide) in a biphasic mixture of MTBE and 10 N aq NaOH (Scheme 7). After 1.5 h at 55 °C the reaction mixture showed >99.5% conversion of **8**. Aqueous workup followed by solvent switch from MTBE to ethanol and crystallization from ethanol/water led to the isolation of (*S*)-**10** in good yield (74%) and purity (99.5% purity). This procedure provided an operationally simpler alternative to the originally developed conditions.

Formation of Carbon−Carbon Bond through Suzuki-Coupling. The Suzuki cross-coupling between aryl chloride [(±)-**10**] and boronic acid **7** was initially performed using conditions closely resembling those of literature procedures.[29] Compared to the synthesis of **1**, this coupling reaction appeared to be more challenging, and the newest generation of biphenylphosphine ligands had to be utilized for successful results. Complete conversion was observed using $Pd_2(dba)_3$/S-Phos and K_3PO_4 in dioxane at reflux. The product (±)-**11** was obtained in >95% yield. Subsequently, a number of bases (NaOH, Na_2CO_3, K_2CO_3, K_3PO_4, $KHCO_3$, dicyclohexylamine) and solvents (mixtures of ethanol, 2-MeTHF, *n*-butanol, or 2-propanol with water) were screened in order to (i) eliminate the use of dioxane and (ii) minimize the protodeboronation of **7** leading to *p*-toluic acid. All inorganic bases led to substantial protodeboronation, and deposition of palladium black on the walls was observed prior to achieving complete conversion. In contrast, reactions performed in the presence of dicyclohexylamine were devoid of these two issues. Complete conversion could be obtained within 4 h at 80 °C in a mixture of ethanol/water (4:1 v/v) with minimal protodeboronation (<1%) and palladium black formation. Product isolation was accomplished by formation of a solution of sodium carboxylate using aq NaOH, a polishing filtration, washing of the filtrate with IPAc/heptane to remove dicyclohexylamine, and acidification of the aqueous layer to afford crystalline (±)-**11** (98.4% purity, 93.4 wt %) in 92% yield (Scheme 8).

Scheme 8. **Suzuki-coupling and isolation of (±)-11**

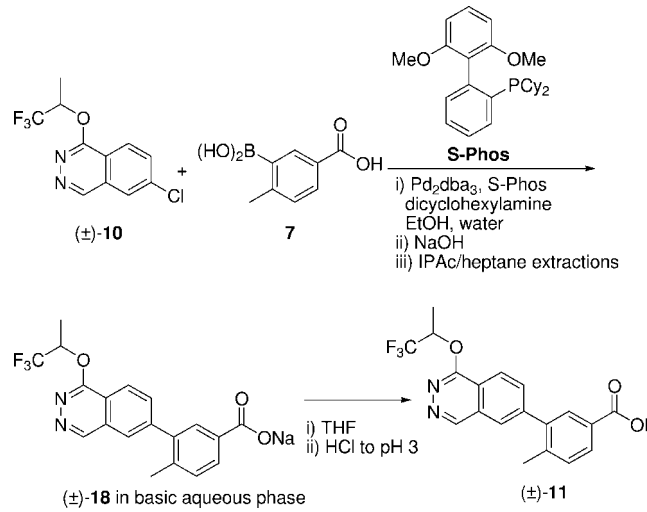

As was the case with intermediate (**10**), a much lower solubility was observed for (*S*)-**11** compared to (±)-**11**.[30] Moreover, the corresponding sodium salt [(*S*)-**18**] also had poor aqueous solubility.[31] The success of the previously developed cross-coupling conditions for the racemic series [$Pd_2(dba)_3$, S-Phos, dicyclohexylamine, aq EtOH] hinged upon an effective two-stage workup: (i) filtration of insoluble byproducts followed by (ii) extractive removal of the dicyclohexylamine freebase. In particular this procedure relied upon a good aqueous solubility of the sodium salt (±)-**18**, which was not preserved for (*S*)-**18**. A modification of the workup by using concentrated NaOH (10 N) was attempted, allowing a complete dissolution of the sodium carboxylate (*S*)-**18** in the ethanol-rich aqueous mixture.[31] This solution was then extracted with heptane to remove dicyclohexylamine. Partial partitioning of ethanol into the heptane/dicyclohexylamine amine layer resulted in supersaturation of the carboxylate and partial product precipitation, which complicated the phase separations. Despite the very favorable reaction profile with dicyclohexylamine as base, the issues in the isolation of (*S*)-**18** required a reevaluation of the base for the Suzuki reaction.

A more extensive screen focused on base (Na_2CO_3, K_2CO_3, Cs_2CO_3, $NaHCO_3$, $KHCO_3$, NaOAc, KOAc, K_3PO_4, K_2HPO_4, NaO^{t}Bu, KO^{t}Bu, dicyclohexylamine)[32] and solvent (ethanol, 1-pentanol, DMF, DMAc, NMP, toluene, methyl isobutyl ketone)[33] while using the same ligand and palladium source [0.25 mol % $Pd_2(dba)_3$, 0.60 mol % S-Phos] as in the previous studies. Only sodium carbonate in aq EtOH performed relatively well when compared to the established dicyclohexylamine-promoted conditions, with protodeboronation being the major side reaction (complete conversion and up to 15 mol % *p*-toluic

(28) The complete data set for the solubility experiments can be found in the Supporting Information.
(29) Barder, T. E.; Walker, S. D.; Martinelli, J. R.; Buchwald, S. L. *J. Am. Chem. Soc.* **2005**, *127*, 4685.
(30) Solubilities of (*S*)-**11** at rt: 6 mg/mL in EtOH, 55 mg/mL in THF, 0.5 mg/mL in water.
(31) Solubilities of the sodium carboxylate [(*S*)-**18**] at rt: >90 mg/mL (EtOH), 61 mg/mL [EtOH/water 1:1 v/v], 3 mg/mL (water).
(32) The same amount of base was used in every reaction (4 equiv). Dicyclohexylamine was used as a control.
(33) Organic solvent (8 vol) with water (2−3 vol).

Scheme 9. **Suzuki-coupling and isolation of (*S*)-11**

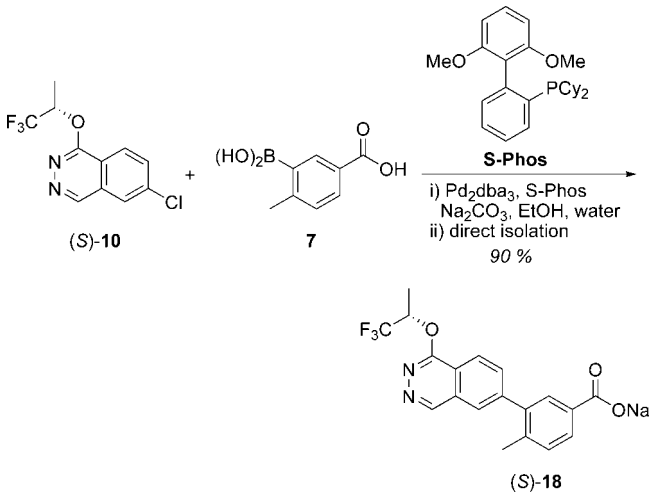

Scheme 10. **Final amide bond formation for the synthesis of (*S*)-2**

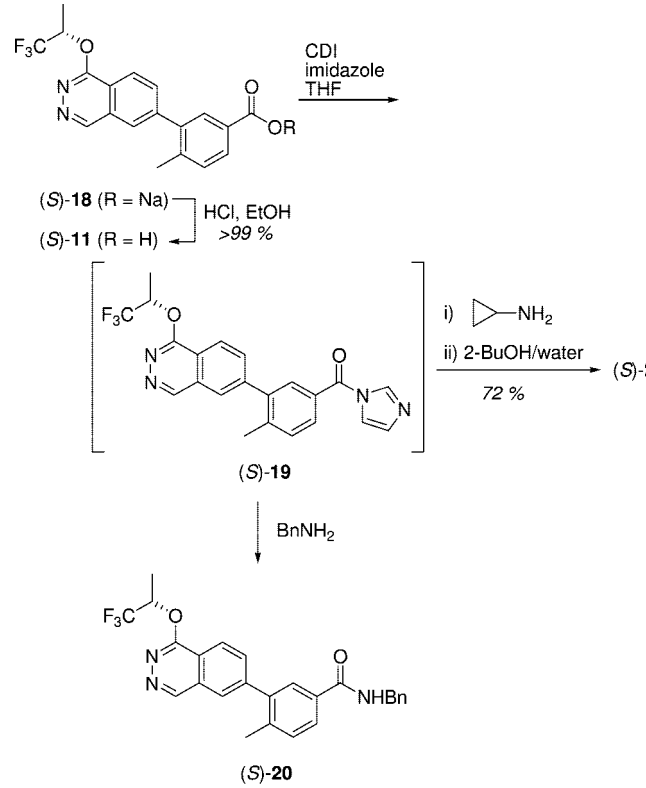

acid). However, under these reaction conditions the poor aqueous solubility of the sodium carboxylate [(*S*)-**18**] could be used advantageously in the isolation. In fact (*S*)-**18** was obtained directly from the postreaction mixture by simple filtration and *p*-toluic acid was rejected to the aqueous ethanol filtrates (Scheme 9). In an optimized protocol, (*S*)-**10** was coupled with **7** (1.2 equiv) in the presence of $Pd_2(dba)_3$ (0.25 mol %), 0.60 mol % S-Phos and Na_2CO_3 (4 equiv) in a mixture of ethanol and water (4:1 v/v). Complete conversion was obtained after 15 h at 78 °C. Precipitation of the sodium salt [(*S*)-**18**] as a crystalline solid was observed during cooling of the postreaction mixture. Additional water was added to increase the recovery, leading to isolation of (*S*)-**18** in good yield and purity (100% purity, 89 wt %, 94% yield). Isolation from water/ethanol (2:1 v/v) provided a good combination of impurity rejection (including *p*-toluic acid and residual palladium) with good product recovery (5−10 mg/mL in supernatant). As a result of a large excess of a common countercation (Na^+), the effective solubility of (*S*)-**18** was significantly lower than the solubility of (*S*)-**18** in pure water/ethanol (2:1 v/v) (34 mg/mL). Meanwhile aryl chloride (*S*)-**10** was only sparingly rejected[34] by this workup; therefore, a high conversion [≤0.5% (*S*)-**10**] in the Suzuki-coupling was critical to achieve a high purity of the cross-coupling product. Due to a significantly higher solubility of (±)-**18** compared to that of (*S*)-**18**, the possibility for an upgrade of the enantiomeric purity during the isolation from aq ethanol was investigated. Starting from **10** of 97.4% ee, a significantly upgraded carboxylate product [(*S*)-**18**, (99.8% ee)] was obtained as expected.

Formation of Carbon−Nitrogen Bond and Isolation of (*S*)-2. All activation attempts through acid chloride formation led to incomplete conversions when applied to the synthesis of **1**. Activation with 1,1-carbonyldiimidazole (CDI) had, however, been very successful, and we therefore refocused our development work on the use of CDI for the amide-coupling in the synthesis of (*S*)-**2**. Direct subjection of sodium carboxylate (*S*)-**18** to CDI activation (1.5 equiv) led to incomplete conversion to the acylimidazolide, and addition of acidic additives (sulfuric acid, pyridinium hydrochloride, or trifluoroacetic acid) did not lead to any significant improvement. Closer examination of the solid-state properties of (*S*)-**18** showed that it was isolated as a hydrate with varying water content. Subjection of a batch of (*S*)-**18** containing 3.8 wt % water (∼1 equiv) to 1.05 equiv of sulfuric acid and 2 equiv of CDI led to complete conversion, showing that the moisture in (*S*)-**18** was responsible for the initially observed low conversion.

Considering the propensity of (*S*)-**18** to form hydrates with varying water content, we decided to introduce an additional isolation step into the synthetic sequence (Scheme 10). In contrast to its sodium salt, free acid (*S*)-**11** was a crystalline high-melting solid (mp 267−268 °C) with little propensity to form hydrates or solvates during the crystallization. While direct isolation of (*S*)-**11** at the end of the Suzuki-coupling had been challenging, the conversion of the sodium salt (*S*)-**18** to the free acid (*S*)-**11** was straightforward. Dissolution of (*S*)-**18** in ethanol was followed by a polishing filtration, and crystallization by addition of hydrochloric acid (1.1 equiv) led to a clean formation of (*S*)-**11**. Dilute hydrochloric acid (0.5 N) was used for this purpose to obtain a final solvent ratio that ensured high recovery (>99% yield, >99.8% purity).[35] No hydrolysis of the acid-sensitive ether linkage in (*S*)-**11** was observed under these conditions. The introduction of this additional isolation point also allowed a significant reduction in the palladium content. Typical levels of palladium observed in (*S*)-**18** directly after the Suzuki reaction were 300−600 ppm, whereas (*S*)-**11** was isolated with 40−80 ppm Pd. This finding allowed avoiding

(34) A reaction at 75 °C reached 95% conversion [5% (*S*)-**10**] after 24 h. No significant rejection of the starting material was observed during the isolation of (*S*)-**18**.

(35) The solubility of **12** in a 1:1 v/v mixture of ethanol/water is 0.2 mg/mL.

Scheme 11. **Optimized synthetic sequence for the synthesis of (*S*)-2**

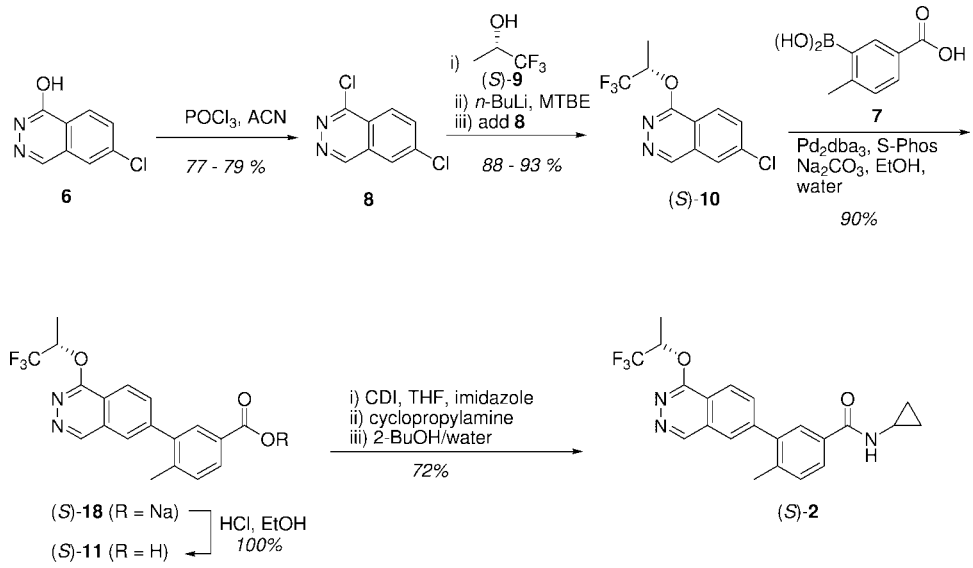

the use of expensive scavenging reagents for the removal of palladium from the API.

Activation of (*S*)-**11** with CDI (1.2 equiv) in THF proceeded without issue. The intermediate acylimidazolide [(*S*)-**19**] was hydrolytically unstable under HPLC conditions (0.1% TFA in acetonitrile/water), but the activation step was monitored by quenching aliquots of the reaction mixture with benzylamine and analyzing quantitatively the resulting benzylamide [(*S*)-**20**]. The activation proceeded well at rt (>95% conversion), but heating at 50 °C for 1 h was required to achieve complete conversion of (*S*)-**11** [<0.5% relative to (*S*)-**20**]. Reaction of the activated intermediate with cyclopropylamine was facile, and complete conversion to (*S*)-**2** [<0.5% (*S*)-**11**] was observed within 1 h at rt. The isolation of (*S*)-**2** was attempted by addition of an antisolvent, but was complicated by the propensity of the system for formation of long cylindrical needles and occasionally that of cotton-like agglomerates. Prolonged time for stirring of the reaction mixture after crystallization led to breaking of the needles, thereby significantly improving the agitation of the mixture. Nonetheless, a balance between product recovery and mechanical properties of the crystallization mixture had to be found. Under optimized conditions, the final solvent composition of tetrahydrofuran/2-butanol and water in a 7:1:6 (v/v/v) ratio was utilized. (*S*)-**2** could be isolated from this mixture in acceptable yield (72%, 22.8 mg/mL loss to mother liquors) and very high purity (>99.9%). More in-depth analysis of the solubility data of (*S*)-**2** in the ternary mixture of tetrahydrofuran/2-butanol and water showed that a moderate decrease in THF content in the final mixture could potentially be used to significantly improve the recovery (up to 20%).[36] This procedure was not adopted for the initial delivery due to concern about the stirrability of the crystallization mixture, but it could potentially be implemented in the design of a more controlled crystallization.[37]

(36) Solubilities of **2**: 23.6 mg/mL in THF/2-butanol/water (50.0/7.2/42.8 v/v/v) and 3.7 mg/mL in THF/2-butanol/water (37.5/8.9/53.6 v/v/v). For additional solubility data in this solvent system see Supporting Information.

(37) A crystallization combined with wet milling should improve the handling properties of (*S*)-**2**.

Summary

A concise synthesis of the p38 MAP kinase inhibitor (*S*)-**2** was developed. The overall sequence involves four synthetic steps from 6-chlorophthalazin-1-ol (**6**) and proceeds in 45% overall yield (Scheme 11). This compares favorable with the 33% overall yield from the more advanced building block 2-chloro-6-bromophthlazine (**3**) in the original synthesis. The developed sequence involves highly efficient reactions for the key constructions of carbon−oxygen, carbon−carbon and carbon−nitrogen bonds. VCD was utilized to correctly assign (*S*)-configuration to the desired enantiomer of **2** prior to initiation of synthetic efforts. PAT (*in situ* Raman spectroscopy) was implemented to monitor the formation of a lithium alkoxide on large scale.

Experimental Section

1,6-Dichlorophthalazine (8). 6-Chlorophthalazin-1-ol (**6**) (2.50 kg, 13.9 mol) and anhydrous acetonitrile (<300 ppm water, 5.8 L) were charged to a 100 L reactor ("reaction vessel"). The jacket temperature was set at 20 °C, and agitation, at 76 rpm. Phosphorus oxychloride (1.94 L, 20.8 mol, 1.50 equiv) was charged to the reaction vessel, and the addition equipment was rinsed with acetonitrile (1.7 L). Reactor contents were then heated to 80 ± 5 °C. After 2 h, a sample was analyzed for reaction completion showing 1.0 HPLC area % of **6** remaining (target ≤2.0%). The reaction vessel contents were cooled to 20 °C over 1.5 h. Sodium phosphate monobasic monohydrate (8.0 g) and sodium phosphate dibasic anhydrous (21.1 g) were dissolved in purified water (15.5 L), and the solution was charged into a 100 L reactor/receiver ("quench vessel") fitted with a pH probe. The reaction mixture was slowly transferred from the reaction vessel into the quench vessel via peristaltic pump, while maintaining the pH at 6.8−8.0 and the batch temperature ≤30 °C. pH adjustment was achieved by simultaneously charging the 2 N NaOH solution during the reaction mixture transfer. A total of 37.0 L of the 2 N NaOH solution was charged over 1.25 h; the final pH was 7.6. Acetonitrile (5.0 L) was charged to the reaction vessel as a rinse and then transferred into the quench vessel. An additional 2.5

L of the 2 N NaOH solution was charged over 15 min; the final pH was 7.5. The quench vessel contents were cooled to 20 °C, and agitation was increased to 120 rpm. The contents of the quench vessel were filtered through a 25 μm polypropylene filter cloth, and the cake was rinsed twice with purified water (2 × 25.0 L). The cake was left under nitrogen blanket and slight vacuum for 4 h. The wet cake was transferred to a vacuum oven and was dried under vacuum with a dry nitrogen sweep at 25 °C until loss on drying (LOD) was ≤1.0% between weighings to afford **8** as an orange crystalline material (2.59 kg, 83.0 wt %, 96.7% purity, 78% yield). The analytical data were in agreement with published data.[5]

(*S*)-6-Chloro-1-(2,2,2-trifluoro-1-methylethoxy)phthalazine [(*S*)-(10)]. (*S*)-1,1,1-Trifluoropropan-2-ol [(*S*)-**9**] in MTBE (91.3 wt %, 1.92 kg, 15.4 mol) and anhydrous MTBE (21.1 L) were charged to a 100 L reactor (alkoxide vessel). The reaction mixture was cooled to 10 ± 5 °C and agitated at 104 rpm. *n*-Butyllithium in hexanes (2.5 M, 23 wt %) was slowly added, while maintaining a batch temperature ≤25 °C (maximum temp 18 °C). During the *n*-butyllithium addition, the reaction was monitored by *in situ* Raman spectroscopy. Complete disappearance of the characteristic alcohol band was observed after addition of 4.00 kg of 23 wt % solution of *n*-butyllithium in hexanes. As confirmation, a small sample was subsequently taken and added into a solution of 1,10-phenanthroline in THF, resulting in a brown indicator solution (excess *n*-butyllithium detected). Additional (*S*)-**9** (91.3 wt %, 196 g, 1.57 mol) was charged to quench any excess *n*-butyllithium in the system. After the second charge, the alcohol peak was again visible by Raman spectroscopy, and the 1,10-phenanthroline test resulted in a colorless indicator solution (no *n*-butyllithium detected). The resulting alkoxide solution was left stirring in the reactor at ≤10 °C. 1,6-Dichlorophthalazine (**8**) (83.0 wt %, 2.54 g, 10.6 mol) and anhydrous MTBE (8.5 L) were charged to a second 100 L reactor (reaction vessel). The reactor jacket temperature was set at 20 °C, and agitation was set at 64 rpm. The alkoxide solution was then transferred from the alkoxide vessel to the reaction vessel over 15 min; final temperature after the addition was 15 °C. Anhydrous MTBE (1.0 L) was charged as a rinse to the alkoxide vessel and was subsequently transferred to the reaction vessel. Once the alkoxide addition was complete, the reactor contents were heated to 45 °C and stirred at 154 rpm. At 1.5 h of elapsed reaction time, a sample analyzed for reaction completion showed 0.29 HPLC area % of starting material **8** remaining (target ≤0.50%). Reactor contents were cooled to 24 °C, and anhydrous THF (10.5 L) was charged to the reactor. A solution of ammonium chloride (0.57 kg) in purified water (4.2 L) was slowly charged to the reactor in small increments over 6 min to control concomitant NH_3 gas evolution. The reactor contents were agitated at 156 rpm for 13 min and then allowed to separate overnight. The contents of the reaction vessel were filtered through a tightly packed pad of Celite 521 (2.0 kg). The pad was rinsed with THF (2.0 L). The biphasic filtrate was collected in a second reactor, heated to 40 °C, agitated for 10 min, and allowed to separate over 30 min. The aqueous layer and the rag layer were discarded. The reactor jacket temperature was set to 70 °C, and ∼30 L of organic distillate was collected under reduced pressure (9.75 psia); the final batch volume was ∼20 L. Ethanol (21.5 L) was charged to the reactor, and the reactor jacket temperature was increased to 80 °C. Twenty-two liters of the contents was distilled off (4.75 psia), and the final batch volume was ∼21 L. Ethanol (10.5 L) was charged to the reactor, and 12 L was distilled (3.5 psia) off to a final batch volume of ∼20 L. The reactor contents were heated to 64 °C. Purified water (10.5 L) was slowly added over 30 min while maintaining a batch temperature of 60 ± 5 °C. Reactor contents were agitated at 250 rpm for 10 min and then cooled to 21 °C over 4 h. After ∼8 h at 21 °C, the contents of the reactor were filtered through a 25 μm polypropylene filter cloth. The cake was rinsed twice with a mixture of ethanol (2.1 L) and purified water (8.4 L). The cake was left under nitrogen blanket and slight vacuum for 5 h. The wet cake was transferred to a vacuum oven and dried under vacuum and nitrogen sweep at 55 °C for ∼48 h to afford **10** as yellow crystals (2.73 kg, 94.8 wt %, 99.6% purity, 90% yield). Mp 135−137 °C; IR 1616, 1583, 1552, 1474, 1457, 1425, 1415, 1398, 1387, 1330, 1274, 1215, 1179, 1170, 1146, 1113, 1072, 1026, 918, 896, 848, 818, 757, 687, 655 cm^{-1}; ^1H NMR (DMSO-d_6, 400 MHz) δ 9.42 (1H, s), 8.34 (1H, d, J = 1.9 Hz), 8.16 (1H, d, J = 8.8 Hz), 8.07 (1H, d, J = 8.8, 1.9 Hz), 6.35−6.22 (1H, m), 1.63 (3H, d, J = 6.4 Hz); ^{13}C NMR (DMSO-d_6, 101 MHz) δ 157.8, 148.3, 137.8, 133.7, 129.7, 125.8, 124.5, 124.4 ($^1J_{CF}$ = 281 Hz), 117.0, 68.9 ($^2J_{CF}$ = 32 Hz), 13.2; HRMS (*m*/*z*): [M + H^+] calcd for ($C_{11}H_9ClF_3N_2O$): 277.0350; Found: 277.0347. Anal. Calcd for $C_{11}H_8ClF_3N_2O$: C, 47.76; H, 2.91; N, 10.13. Found: C, 47.66; H, 2.85; N, 10.14.

Sodium (*S*)-4-Methyl-3-[1-(2,2,2-trifluoro-1-methylethoxy)phthalazin-6-yl]benzoate [(*S*)-(18)]. (*S*)-6-Chloro-1-(1,1,1-trifluoropropan-2-yloxy)phthalazine [(*S*)-**10**] (94.8 wt %, 2.73 kg, 9.37 mol), 3-carboxy-6-methylphenylboronic acid (**7**) (92.9 wt %, 2.36 kg, 12.2 mol), sodium carbonate (3.97 kg, 37.5 mol), and ethanol (21.0 L) were charged to a 100 L reactor. Purified water (5.2 L) was charged, and the reactor was vacuum purged twice by evacuating the vessel to ∼11 psia and then bringing the pressure up to ∼15.5 psia with nitrogen. 2-Dicyclohexylphosphino-2′,6′-dimethoxy-1,1′-biphenyl (S-Phos, 23.1 g, 0.056 mol) and tris(dibenzylideneacetone)dipalladium(0) (21.4 g, 0.023 mol) were charged as slurries in ethanol (0.75 L each) to the reactor. The reactor was vacuum purged twice by evacuating the vessel to ∼11 psia and then bringing the pressure up to ∼15.5 psia with nitrogen. The reaction mixture was heated to 80 ± 10 °C and agitated at 133 rpm. After ∼17 h, a sample was analyzed for reaction completion showing ≤0.05 HPLC area % of (*S*)-**10** remaining (target ≤0.50%). The reactor contents were cooled to 65 °C and purified water (37.0 L) was charged to the reactor while maintaining a batch temperature ≥48 °C. The reactor contents were then cooled to 24 °C over 2.5 h with agitation at 180 rpm. The contents of the reactor were filtered through a 25 μm polypropylene filter cloth. The cake was rinsed twice with purified water (2 × 13.0 L). The cake was left under nitrogen blanket and slight vacuum for 4.5 days to afford (*S*)-**18** as an off-white crystalline material (4.98 kg, 67.1 wt %, 99.9% purity, 90% yield). Mp 90−92 °C; IR 3288, 1612, 1582, 1543, 1437, 1390, 1333, 1169, 1153, 1110, 1081, 1027, 909,7, 848, 785, 677 cm^{-1}; ^1H NMR (DMSO-d_6, 400 MHz) δ 9.48 (1H, s), 8.20 (1H, d, J = 8.4 Hz), 8.16 (1H,

s), 8.05 (1H, dd, J = 8.4, 1.5 Hz), 7.87 (1H, dd, J = 8.0, 1.9 Hz), 7.84 (1H, s), 7.27 (1H, d, J = 8.2 Hz), 6.37−6.25 (1H, m), 2.26 (3H, s), 1.64 (3H, d, J = 6.4 Hz); ^{13}C NMR (DMSO-d_6, 101 MHz) δ 169.1, 158.0, 149.3, 146.8, 138.9, 138.2, 135.0, 134.6, 130.6, 129.6, 129.1, 128.9, 126.2, 124.6 ($^1J_{CF}$ = 281 Hz), 121.7, 117.1, 68.7 ($^2J_{CF}$ = 32 Hz), 19.9, 13.3; HRMS (*m*/*z*): [M + H$^+$] calcd for ($C_{19}H_{15}F_3NaN_2O_3$): 399.0927; Found: 399.0917.

(*S*)-4-Methyl-3-[1-(2,2,2-trifluoro-1-methylethoxy)phthalazin-6-yl]benzoic acid [(*S*)-(11)]. Sodium (*S*)-4-methyl-3-(1-(1,1,1-trifluoropropan-2-yloxy)phthalazin-6-yl)benzoate [(*S*)-**18**] (4.98 kg) and ethanol (25.0 L) were charged to a reactor. Agitation at 100 rpm was applied until complete dissolution was achieved. A sample of the solution analyzed for the net content of (*S*)-**18** showed 3.34 kg (8.38 mol) of (*S*)-**18** in solution. The direct determination of the potency of solid (*S*)-**18** was challenging due to sampling heterogeneity; the acid charge was therefore based on the assay in solution. The solution was filtered through a 5 μm polypropylene filter into a second reactor. The reactor jacket temperature was set at 20 °C and agitation at 158 rpm. While the batch temperature was maintained at ≤30 °C, 0.5 N HCl (18.4 L, 9.20 mol) was slowly charged to the reactor. The reactor contents were then cooled to 20 ± 5 °C and stirred at 156 rpm. After aging for 1 h the reactor contents were filtered through a 25 μm polypropylene filter cloth. The cake was rinsed three times with a mixture of ethanol/water (1:1, 13.0 L). The cake was left under nitrogen blanket and slight vacuum for 16 h. The wet cake was transferred to a vacuum oven and dried under vacuum and nitrogen sweep at 55 °C for ∼48 h to afford (*S*)-**11** as a crystalline white solid (3.18 kg, 100.8 wt %, 100.0% purity, 100% yield). Mp 268−270 °C; IR 3352, 1627, 1574, 1402, 1390, 1300, 1268, 1257, 1238, 1182, 1156, 1077, 1028, 842, 763, 703, 679 cm^{-1}; ^{1}H NMR (DMSO-d_6, 400 MHz) δ 13.01 (1H, s), 9.47 (1H, s), 8.24−8.20 (2H, m), 8.08 (1H, dd, J = 8.6, 1.4 Hz), 7.95 (1H, dd, J = 8.0, 1.8 Hz), 7.87 (1H, s), 7.52 (1H, d, J = 8.0 Hz), 6.36−6.25 (1H, m), 2.36 (3H, s), 1.64 (3H, d, J = 6.5 Hz); ^{13}C NMR (DMSO-d_6, 101 MHz) δ 166.9, 158.0, 149.2, 145.1, 140.4, 139.7, 134.3, 131.0, 130.4, 129.1, 128.9, 126.5, 125.1 ($^1J_{CF}$ = 281 Hz), 121.9, 117.4, 68.7 ($^2J_{CF}$ = 32 Hz), 20.2, 13.2; HRMS (*m*/*z*): [M + H$^+$] calcd for ($C_{19}H_{16}F_3N_2O_3$): 377.1108; Found: 377.1098.

(*S*)-*N*-Cyclopropyl-4-methyl-3-[1-(2,2,2-trifluoro-1-methylethoxy)phthalazin-6-yl]benzamide [(*S*)-(2)]. (*S*)-4-Methyl-3-(1-(1,1,1-trifluoropropan-2-yloxy)phthalazin-6-yl)benzoic acid [(*S*)-(**11**)] (3.01 kg, 7.99 mol), imidazole (274 g, 4.02 mol) and THF (18.0 L) were charged to a reactor. Jacket temperature was set at 20 °C and agitation at 122 rpm. 1,1′-Carbonyldiimidazole (CDI, 1.56 kg, 9.64 mol) was slowly charged to the reactor in portions to control gas evolution, and the reactor contents were then heated to 50 ± 5 °C. After 1 h at temperature, a sample was quenched with benzylamine and analyzed for reaction completion, showing 0.30 HPLC area % of (*S*)-**11** remaining (target ≤0.50%). The reactor contents were cooled to 22 °C, and the reaction solution was transferred through a 5 μm polypropylene filter into a second reactor. THF (3.0 L) was charged to the reactor as a rinse and then transferred through the same 5 μm polypropylene filter into the second reactor. Reactor agitation was set at 131 rpm and jacket temperature at 20 °C. Cyclopropylamine (1.12 L, 16.2 mol) was charged to the reactor over 18 min while maintaining a batch temperature ≤30 °C. After 1 h a sample analyzed for reaction completion showed 0.26 HPLC area % of (*S*)-**11** remaining (target ≤0.50%). A solution of 2-butanol (3.0 L) and purified water (18.0 L) were charged to the reactor over 30 min; agitation was set at 180 rpm. The contents of the reactor were filtered through a 10 μm polypropylene filter cloth. The wet cake was washed with three portions of a THF/water mixture (1/3 v/v, 28.0 L total). The cake was left under nitrogen blanket and slight vacuum for 19 h. The wet cake was transferred to a vacuum oven and dried under vacuum at 50 °C for ∼48 h to afford (*S*)-**2** as crystalline white solid (2.37 kg, 100.1 wt %, 100.0% purity, 72% yield). Mp 200−202 °C; IR 1651, 1539, 1492, 1432, 1392, 1268, 1184, 1153, 1127, 1109, 1081, 1024, 849, 763, 677 cm^{-1}; ^{1}H NMR (DMSO-d_6, 400 MHz) δ 9.48 (1H, s), 8.46 (1H, d, J = 3.9 Hz), 8.25−8.20 (2H, m), 8.09 (1H, dd, J = 8.4, 1.4 Hz), 7.84 (1H, dd, J = 7.8, 1.6 Hz), 7.81 (1H, s), 7.46 (1H, d, J = 8.0 Hz), 6.38−6.25 (1H, m), 2.89−2.81 (1H, m), 2.30 (3H, s), 1.64 (3H, d, J = 6.5 Hz), 0.73−0.66 (m, 2H), 0.59−0.54 (m, 2H); ^{13}C NMR (DMSO-d_6, 101 MHz) δ 166.8, 158.0, 149.2, 145.5, 139.3, 138.3, 134.5, 132.3, 130.6, 128.8, 128.4, 127.1, 126.5, 124.6 ($^1J_{CF}$ = 281 Hz), 121.8, 117.3, 68.7 ($^2J_{CF}$ = 32 Hz), 23.0, 20.0, 13.3, 5.7; HRMS (*m*/*z*): [M + H$^+$] calcd for ($C_{22}H_{21}F_3N_3O_2$): 416.1580; Found: 416.1574.

Acknowledgment

We thank Dr. M. J. Martinelli, Dr. M. M. Faul, Dr. A. S. Tasker, Dr. D. Zhang, and Dr. L. Pettus for valuable discussions on the synthesis of the target compound. Dr. J. Preston, Dr. T. Yan, J. Chen, C. Scardino, Dr. P. Grandsard, Dr. T. Wang, B. Shaw, Dr. B. Shen, Dr. J. Ostovic, M. Petkovic, M. Ronk, Dr. K. Turney, and M. Wacker are thanked for analytical support. Dr. P. Schnier and R. Stanton are gratefully acknowledged for providing the spectral convolution routine. Dr. A. Gore and Dr. K. Nagapudi are thanked for help in solid-state characterization. J. Manley, J. Clare, Dr. K. McRae, J. Tvetan, J. Tomaskevitch, S. Huggins, B. Southern, and G. Sukay are thanked for support and valuable input during scale-up.

Supporting Information Available

Copies of ^{1}H NMR and ^{13}C NMR spectra for compounds (*S*)-**2**, (*S*)-**10**, (*S*)-**11**, **16**, (*S*)-**18** and (*S*)-**20**; additional experimental procedures and characterization data for compounds (*S*)-**13**, (*S*)-**9**, (*S*)-**10**, and (*S*)-**20**; additional details concerning the VCD experiments, the experiments for generation of the ternary phase diagram of **10**, and solubility data for (*S*)-**2**. This material is available free of charge via the Internet at http://pubs.acs.org.

Received for review October 1, 2008.

OP800250V